HiSOR

ACTIVITY REPORT

2015

Hiroshima Synchrotron Radiation Center, HiSOR
Hiroshima University

HiSOR
ACTIVITY REPORT

2015

Hiroshima Synchrotron Radiation Center, HiSOR

Hiroshima University

Edited by H. Sato

The annual report is available from

Hiroshima Synchrotron Radiation Center, Hiroshima University
Kagamiyama 2-313, Higashi-Hiroshima 739-0046, JAPAN

Phone: +81-82-424-6293
Fax: +81-82-424-6294
e-mail: hisor@hiroshima-u.ac.jp
URL: http://www.hsrc.hiroshima-u.ac.jp/

Preface

Hiroshima Synchrotron Radiation Center (HiSOR), Hiroshima University, celebrated its 20-year anniversary ceremony and held the 20th international symposium on synchrotron radiation on March 10 and 11, 2016.

We are promoting research in materials science using synchrotron radiation from ultraviolet (VUV) to soft x-ray region. In particular, high-resolution electronic structural analysis using high-brightness ultraviolet undulator emission and the structural analysis biomaterial in water using circularly polarized VUV are attracting much international cooperative research.

HiSOR is a Joint Usage/Research Center, which is a national cooperative research system to promote joint research since 2004. External evaluations were conducted for the activities of joint research/joint use in 2015, and we achieved an A-rank score.

HiSOR has promoted high-resolution electronic structure analysis and the improvement of related techniques. BL1, a linear undulator beam line, enables linear-polarization-dependent measurements using a rotatable photoemission spectrometer. BL9A, an Apple II-type variable polarization undulator beam line, the improvement of normal incidence monochromator and the replacement of the magnetic shield vacuum chamber to mount new motorized 6 axis low temperature goniometer were conducted. Furthermore, a new laser system has been introduced as an advanced VUV light system to enhance synchrotron radiation experiments. BL9B, the branch beam line of the Apple-II undulator, is three-dimensional spin-resolved ARPES beam line. The electron energy analyzer incorporating two new high-efficiency spin detectors has enabled the visualization of spin dependent electronic states.

The number of cooperative researchers not from Hiroshima University was 125 (49 researchers were from foreign countries) from 39 institutions in 2015. The number of research institutions, which has the researchers using HiSOR, is 48 (overseas) and 54 (in Japan) since 2004.

Finally, I thank all users of HiSOR and other related research institutions and appreciate the financial support of the Joint Usage/Research Center project of MEXT.

September 2016
Hirofumi Namatame
Director for Hiroshima Synchrotron Radiation Center

Hirofumi Namatame

Table of Contents

Appendices

Current Status of HiSOR

Status of the HiSOR storage ring

1. Introduction

The HiSOR is a synchrotron radiation (SR) source of Hiroshima Synchrotron Radiation Center, Hiroshima University, established in 1996. It is a compact racetrack-type storage ring having 21.95 m circumference, and its natural emittance of 400π nmrad is rather large compared with those of the other medium to large storage rings. The most outstanding advantage of the facility lies in good combination with state-of-the-art beamlines (BL's) for high-resolution photoelectron spectroscopy in the photon energy ranges between VUV and soft X-ray. The principal parameters of HiSOR are shown in Table 1.

Table 1: Main parameters of the HiSOR Storage ring.

Circumference	21.95 m
Type	Racetrack
Bending radius	0.87 m
Beam energy at Injection	150 MeV
at Storage	700 MeV
Magnetic field at Injection	0.6 T
at Storage	2.7 T
Injector	150 MeV Racetrack Microtron
Betatron tune (ν_x, ν_y)	(1.72, 1.84)
RF frequency	191.244 MHz
Harmonic number	14
RF voltage	200 kV
Stored current (nominal)	350 mA
Natural emittance	400π nmrad
Beam life time	~10 hours@200 mA
Critical wavelength	1.42 nm
Photon intensity (5 keV)	1.2×10^{11} /sec/mr^2/0.1%b.w./300mA

The originally designed maximum stored current of HiSOR was 300 mA. However, after the improvement of the control system and the RF system in 2003, HiSOR has been in operation with 350 mA maximum stored current since. Fig. 1 shows an example of typical one-day operation. Beam injection for HiSOR is executed twice a day, at around 9:00 and 14:30.

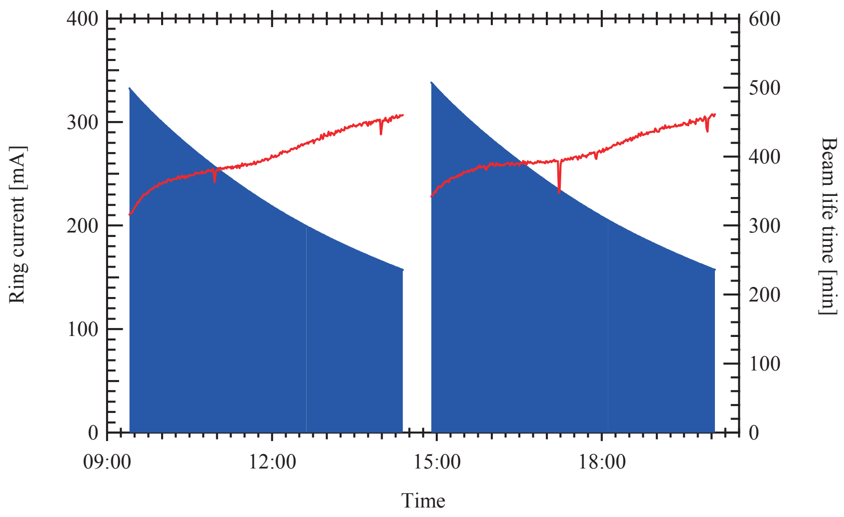

Fig. 1: Typical daily operation status.

HiSOR has two 180-deg. Normal-conducting bending magnets which generate a strong magnetic field of 2.7 T. This storage ring is equipped with two insertion devices, a linear undulator and a quasi-periodic APPLE-II undulator which replaced to the previous helical undulator in summer 2012. Major parameters of these undulators are listed in Table 2. The photon energy spectra of the SR from HiSOR are shown in Fig. 2.

Table 2: Main parameters of the undulators.

Linear undulator (BL-1)	
Total length	2354.2 mm
Periodic length λu	57 mm
Periodic number	41
Pole gap	30-200 mm
Maximum magnetic field	0.41 T
Magnetic material	Nd-Fe-B (NEOMAX-44H)
Quasi-Periodic APPLE-II undulator (BL-9A,B)	
Total length	1845 mm
Periodic length λu	78 mm
Periodic number	23
Pole gap	23-200 mm
Maximum magnetic field	0.86 T (horizontal linear mode)
	0.59 T (vertical linear mode)
	0.50 T (helical mode)
Magnetic material	Nd-Fe-B (NEOMAX-46H)

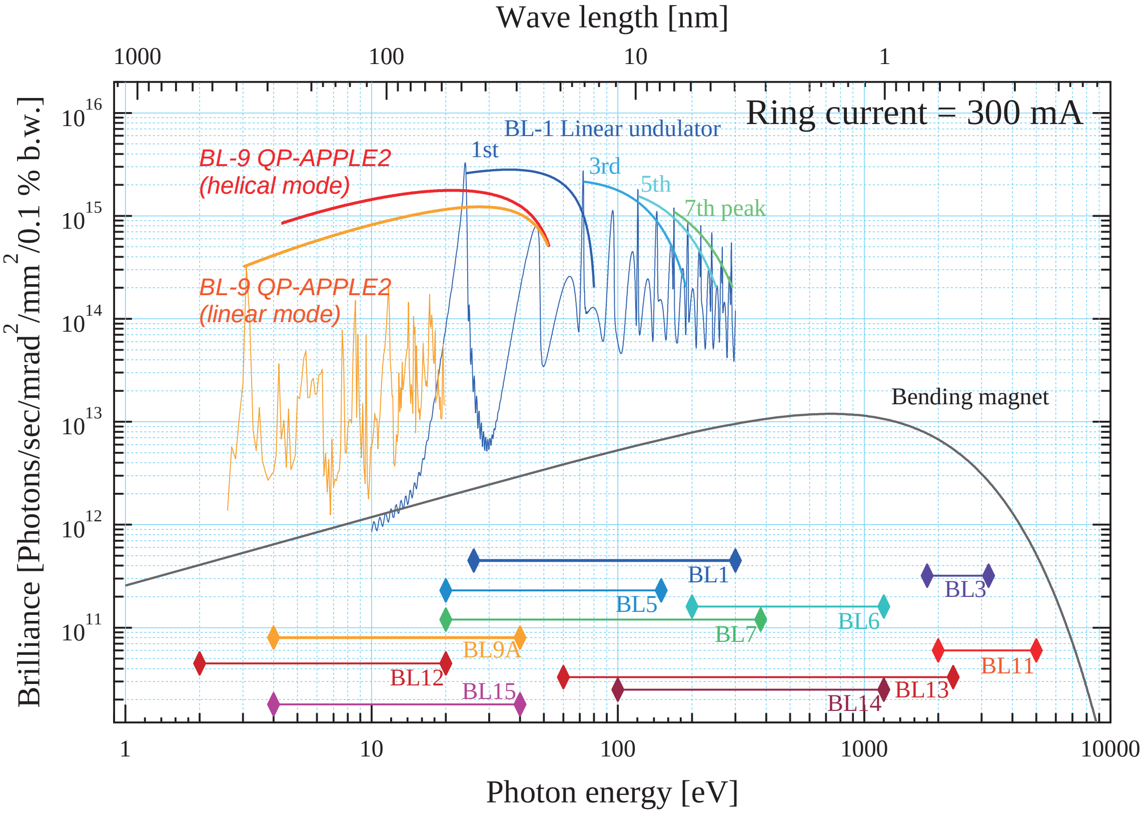

Fig. 2: Photon energy spectra of the SR from HiSOR.

2. Operation status in FY 2015

Fig. 3 shows monthly operation time of HiSOR storage ring in FY 2015. HiSOR has a long term cease period to have routine inspections in summer every year. The total user time of FY2015 achieved 1338 hours. Fig. 4 shows bar graph of total operation days in each fiscal year. It shows that days for user operation in FY2015 was the highest for the last decade. Operation times of the storage ring and the Microtron from FY 2006 to FY 2015 are shown in Fig. 5.

To solve the problem of the water leakage from the absorber completely (see ‘HiSOR Activity Report 2014’ in detail), a new absorber was constructed with an improved design. It was installed during the regular maintenance period at the summer shutdown. Because of recovering the degree of vacuum, commissioning operation of the storage ring was additionally needed in October and the first week in November. As the result, the operation time and user time was gradually recovered at the end of this fiscal year.

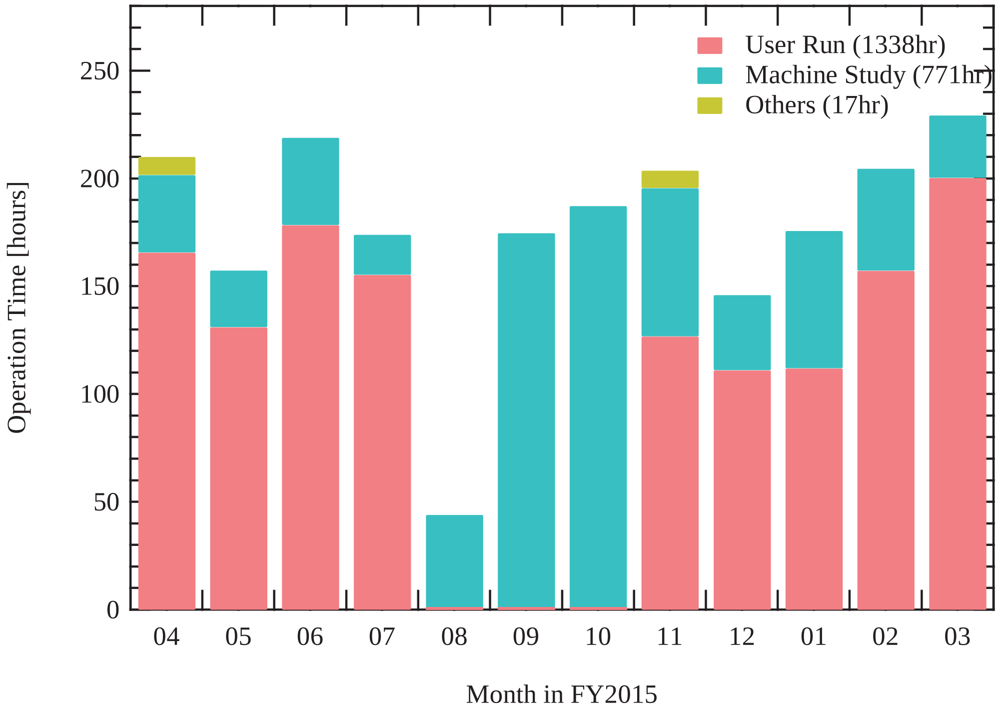

Fig. 3: Monthly operation time in FY 2015.

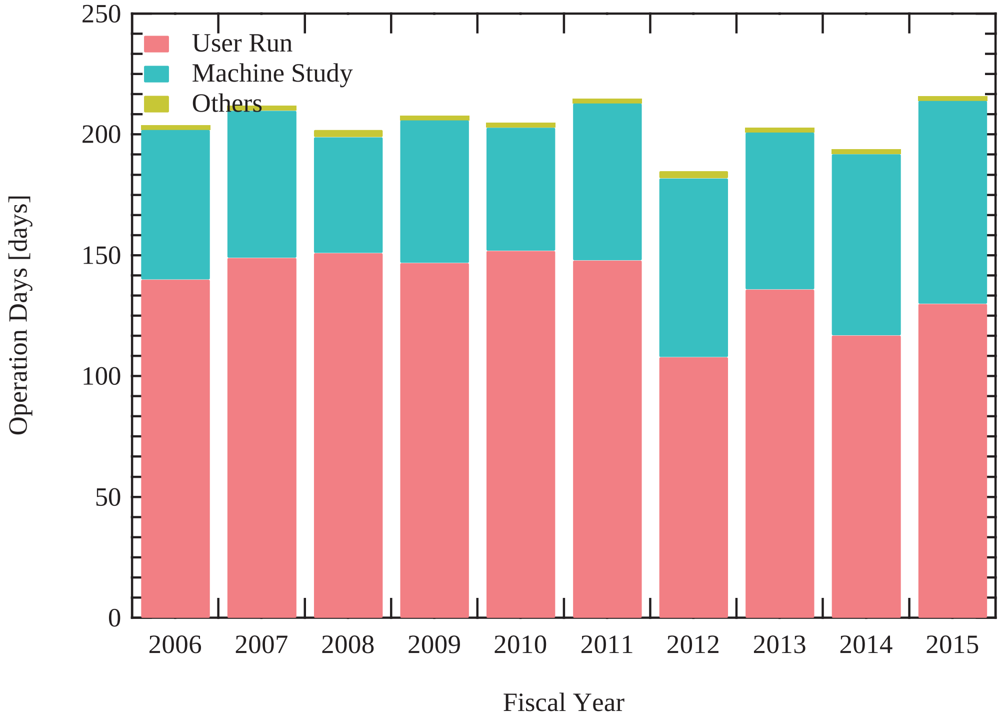

Fig. 4: Operation days of HiSOR storage ring.

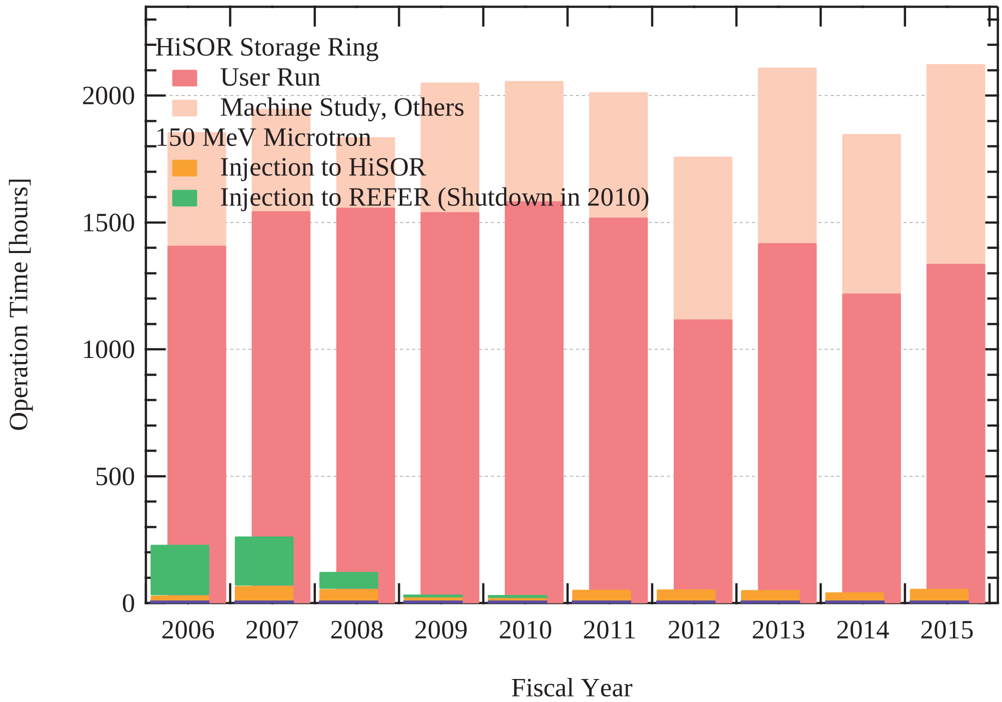

Fig. 5: Annual operation time of Storage ring and Microtron.

Beamlines

A total of 13 beamlines has been constructed so far; three normal-incidence monochromators, seven grazing-incidence monochromators, two double crystal monochromators and apparatus for white beam irradiation (Fig. 1). Table 1 lists the beamlines at present together with the main subject, energy range and monochromators.

Table 1: List of Beamlines

beamline	source	monochro-mator	subject	energy range (eV)	status
BL-1	LU	GIM	Polarization dependent high-resolution ARPES	22-300	in use
BL-3	BM	DCM	Surface XAFS	1800-3200	in use
BL-4	BM		White beam irradiation		closed
BL-5	BM	GIM	ARPES and PEEM	40-220	in use
BL-6	BM	GIM	Gas-phase photochemistry	200-1200	in use
BL-7	BM	GIM	ARPES	20-380	in use
BL-8	BM		Beam diagnosis		
BL-9A	HU/LU	NIM	UV-VUV high-resolution ARPES	5-35	in use
BL-9B	HU/LU	GIM	High-resolution spin-resolved ARPES	16-300	in use
BL-11	BM	DCM	XAFS	2000-5000	in use
BL-12	BM	NIM	VUV-CD of biomaterials	2-10	in use
BL-13	BM	GIM	Surface photochemistry	60-1200	in use
BL-14	BM	GIM	Soft-XMCD of nano-materials	400-1200	in use
BL-15	BM	NIM	VUV-CD of biomaterials	4-40	closed
BL-16	BM		Beam profile monitor		

At present, nine beamlines BL1, BL3, BL6, B7, BL9A, BL9B, BL11, BL12, BL13 and BL14 are opened for users. Furthermore, three off-line systems, spin- and angle-resolved photoemission (SARPES) spectrometer, inverse-photoemission (IPES) spectrometer and low-temperature scanning tunneling microscope (LT-STM) system have also opened for users (Fig. 2).

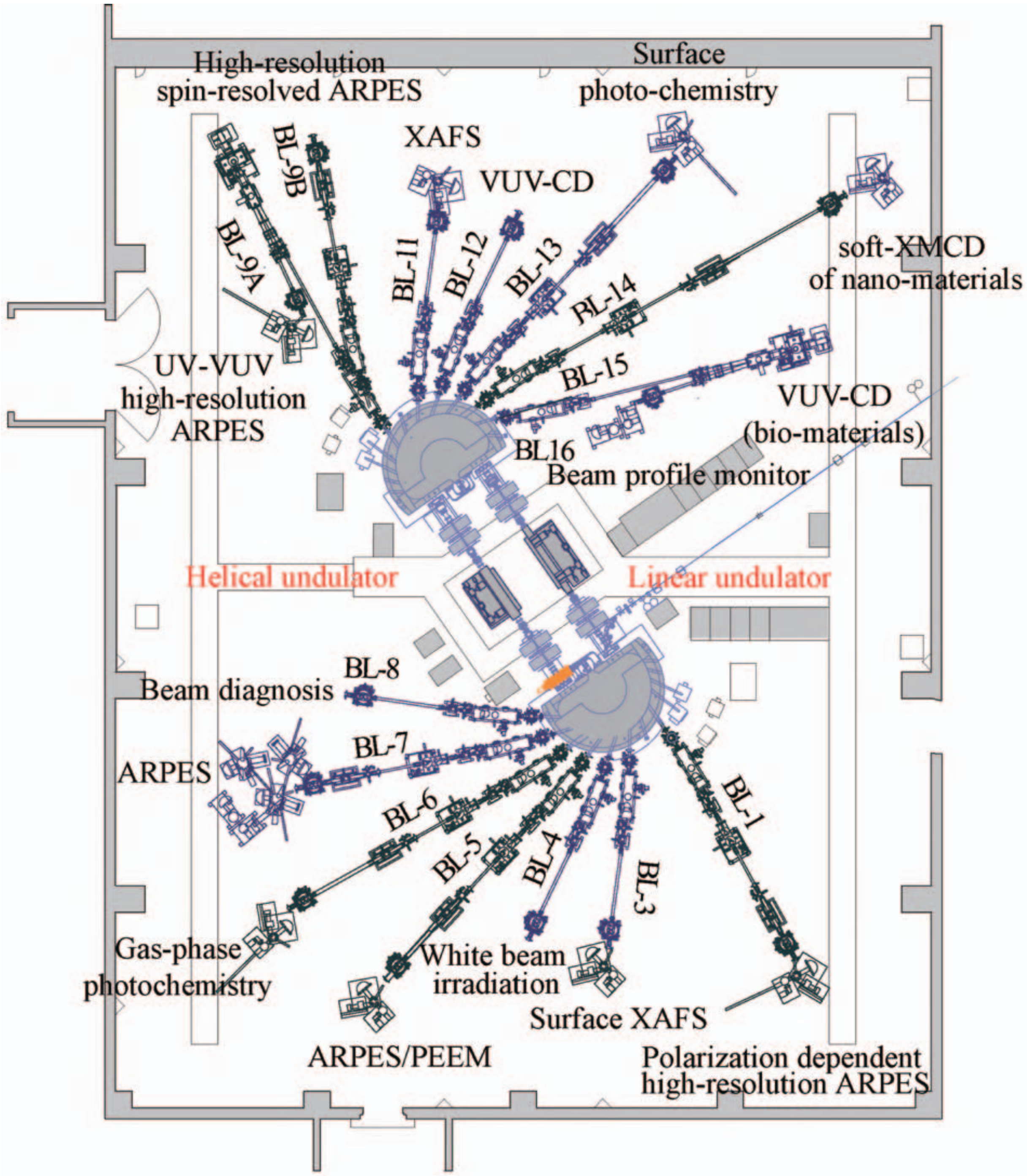

Fig. 1: Schematic view of the experimental hall.

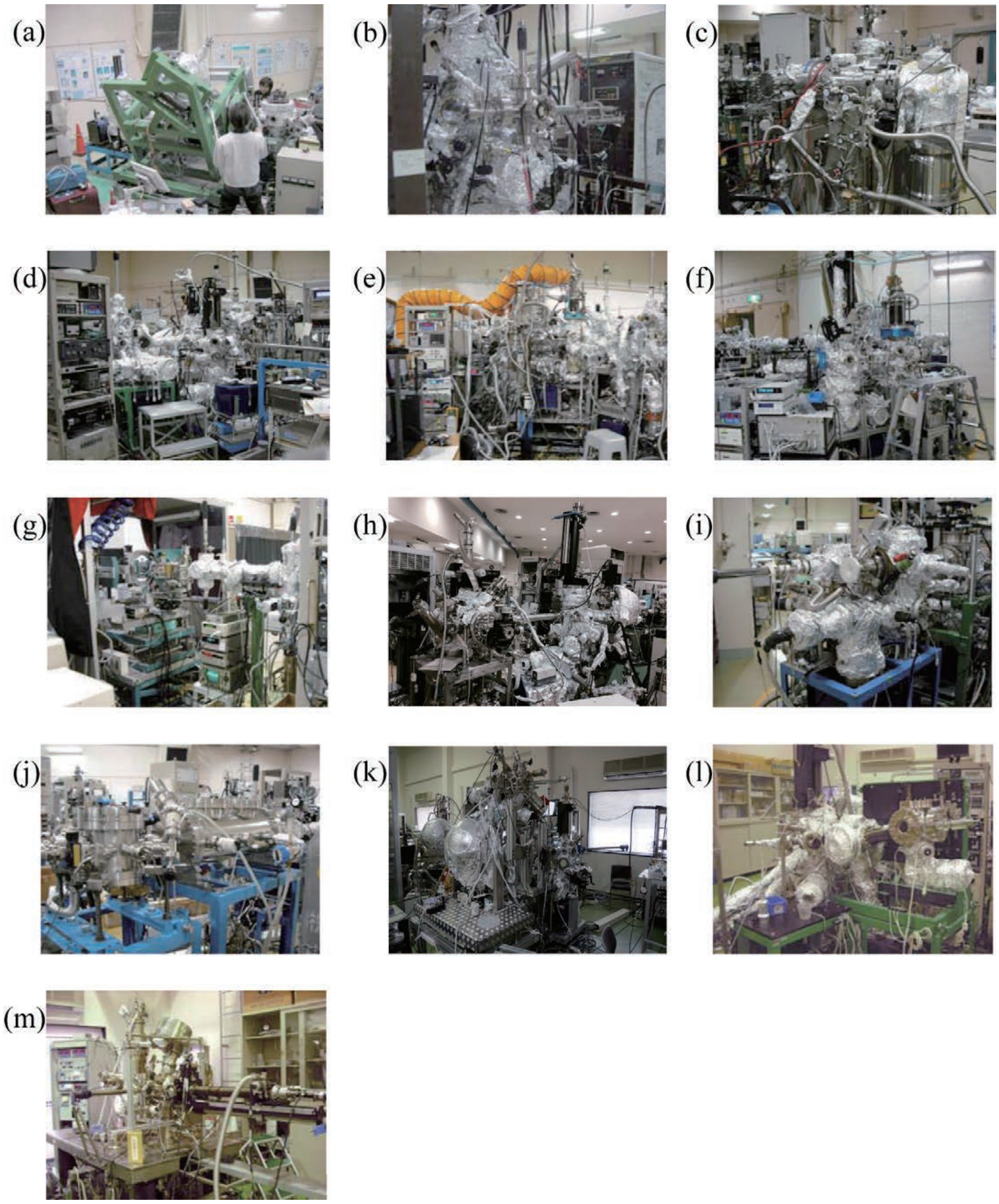

Fig. 2: Experimental apparatus for Joint usage and Joint research. (a) BL-1, (b) BL-3, (c) BL-6, (d) BL-7, (e) BL-9A, (f) BL-9B, (g) BL-11, (h) BL-13, (i) BL-14, (j) BL-12, (k) Spin resolved photoemission (offline), (l) Resonant inverse photoemission (offline), (m) LT-STM (offline).

Research Activities

– Accelerator Studies –

Magnetic design of Knot-APPLE undulator and its performance

Nobumitsu Kawata[a] and Shigemi Sasaki[b]

[a]*Department of Physical Science, Graduate School of Science, Hiroshima University*
[b]*Hiroshima Synchrotron Radiation Center, Hiroshima University*

Keywords: undulator

In order to generate a low energy photon beam in a high energy storage ring with an insertion device, it is necessary to increase the undulator's deflection parameter, *K*. If this is the case, a high heat load on beamline elements is a serious problem because the on-axis radiation power increases drastically as increasing the value of *K* parameter for a linear undulator. To reduce the on-axis heat load, the Figure-8 undulator, the Knot undulator and other exotic undulators were proposed [1-4].

In a Figure-8 undulator, the period length of horizontal magnetic field is twice as large as that of vertical field, and hence the projected beam orbit draws a figure of number 8. The direction of velocity vector of electrons always deviates from the undulator axis, and projected motion of electrons draws alternately a clockwise and anti-clockwise orbit, which results in the cancellation of circular polarization of the photons and leaves a remanent linear polarization.

In a Knot undulator, the magnetic field period in horizontal direction is 1.5 times larger than that of the vertical direction, and hence the undulator period is 3 times larger. The direction of velocity vector never coincides to but rather always deviates from the undulator axis. The spatial distribution of corresponding power density draws a knot-like figure.

However, neither Figure-8 nor Knot udulator has the capability to change polarizations. On the other hand, the APPLE undulator is capable to generate variable polarization, but is not capable to reduce on-axis power density in linear modes. We propose a novel Knot-APPLE undulator which is capable to reduce an on-axis high heat load and generate every polarization state.

Firstly, we designed Knot-APPLE undulator for Shanghai Synchrotron Radiation Facility (SSRF). Figure 1 and 2 show magnet structure of Knot-APPLE undulator. Second, we modified magnet structure suitable for low energy storage ring such as the HiSOR-II ring to evaluate the performance of Knot-APPLE undulator.

Figure 3 and 4 show examples of magnetic field distribution and expected angular power distributions, respectively.

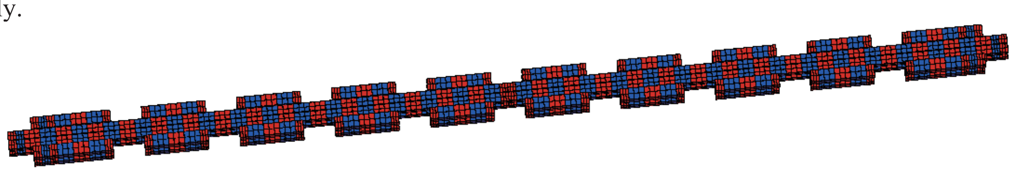

FIGURE 1. This is the RADIA model of magnet structure for a Knot-APPLE undulator.

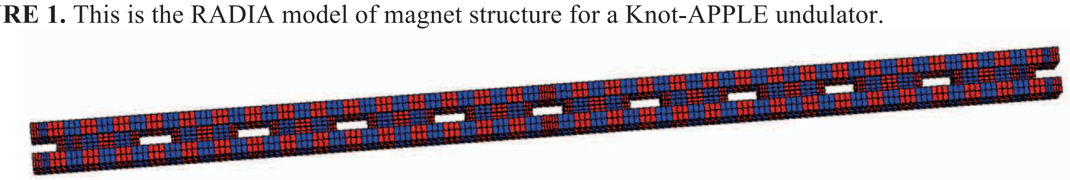

FIGURE 2. Another RADIA model of magnet structure for a Knot-APPLE undulator.

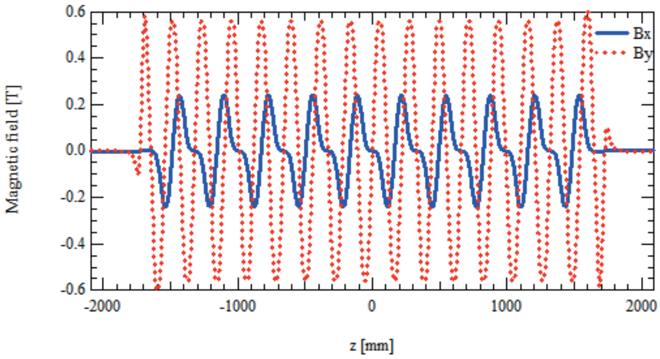

FIGURE 3. Magnetic distribution of Knot-APPLE undulator (horizontal linear mode).

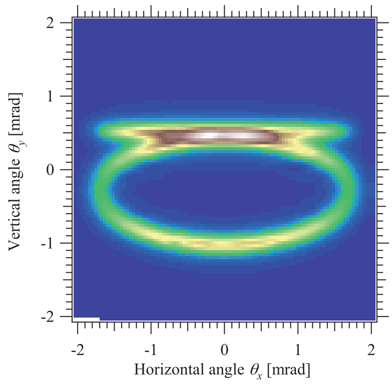

FIGURE 4. Angular power distribution of Knot-APPLE undulator (horizontal linear mode).

Expected radiation spectra and power densities of various mode for Knot-APPLE undulator are presented in the presentation.

REFERENCES

1. T. Tanaka and H. Kitamura, Nucl. Instrum. Meth. A364, 368 (1995).
2. S. Sasaki, B. Diviacco, R.P. Walker, Proc. EPAC98, pp.2237, 1998.
3. S. Sasaki, "Undulators, wigglers and their applications," pp.237-243 (Ed. by H. Onuki and P. Elleaume, Taylor & Francis Inc, New York, 2003), and Proc. Of NAPAC 2013, WEPSM01, p. 1043, Pasadena, CA (2013).
4. S. Qiao, *et al*., Rev. Sci. Instrum., 80, 085108 (2009).

Sound of Quasi-Periodic Undulator

Yuya Ichioka[a] and Shigemi Sasaki[b]

[a]*Department of Physical Science, Faculty of Science, Hiroshima University*
[b]*Hiroshima Synchrotron Radiation Center, Hiroshima University*

Keywords: Undulator

The synchrotron radiation generated by a periodic linear undulator contains higher harmonics of integral multiple of fundamental harmonic in the spectrum. These higher harmonics are usually harmful for user's experiments. In many cases, it is not so easy to eliminate unwanted higher harmonics by using conventional optical elements such as a single grating monochrometer. In order to solve this problem, a scheme of QPU(Quasi-Periodic Undulator) was proposed. The QPU is realized by modifying the magnetic structure so that the sequence of phase slip in each half period is corresponding to the order of quasi-periodicity. A conventional QPU is realized by introducing a smaller phase slip at appropriate positions in a periodic undulator. A new type QPU can be realized by introducing a larger phase slip. Figure 1 shows the magnetic field distribution for two different types of QPU. The light spectral features of two different types of QPU are shown in Fig.2.

(a) (b)

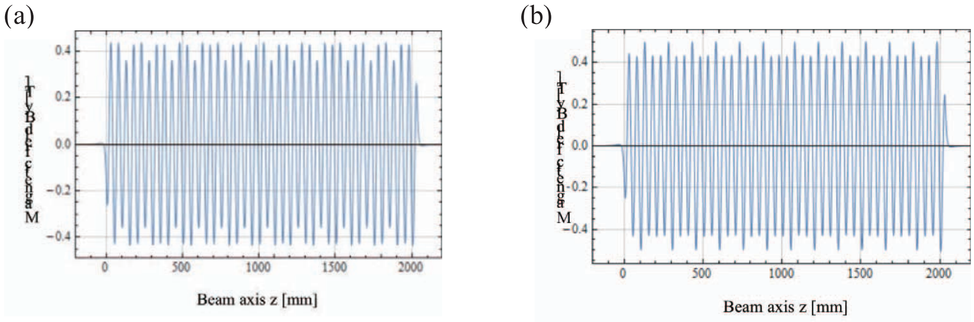

Fig.1. Magnetic field distribution (a) conventional QPU, (b) new type QPU

(a) (b)

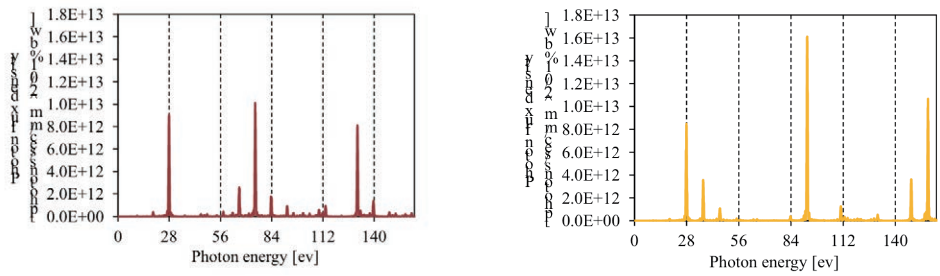

Fig.2. Radiation spectrum (a) conventional QPU, (b) new type QPU

For the intuitive grasp of differences between two undulators, there is a method of converting the light spectrum to the sound. The light is a transverse wave propagating in vacuum. The sound is longitudinal wave propagating in the medium. The light and sound are considered equivalent in terms of vibration felt by the five senses. In this study, we convert the light spectrum to the sound in the audible range, and investigate the possibility to clearly distinct the differences in spectrum. Figure.3 shows waveform of sound normalized by the first harmonic. These results indicate that the spectral differences of radiation spectra can be clearly distinguished by hearing the sound.

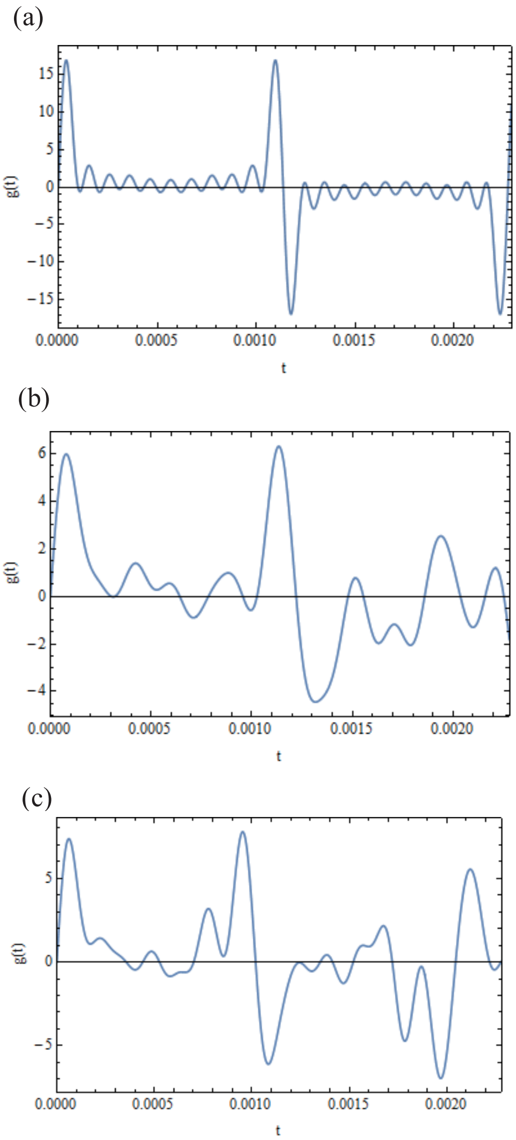

Fig.3. Wave forms of (a) periodic undulator, (b) conventional QPU, and (c) strong field QPU radiations

REFERENCES

1. S.Hashimoto and S.Sasaki, Nucl. Instr. Methods in Phys. Res. A361,611 (1995).
2. S.Sasaki, et.al, Proceedings of EPAC’98, p.2237, Stockholm, Sweden, 1998.
3. S.Sasaki, Proceedings of IPAC’10, P.3141, Kyoto, Japan, 2010.

Design for New Type Quasi-Periodic Undulator

Hatsuya Mima[a], and Atsushi Miyamoto[b], Shigemi Sasaki[c]

[a]Department of Pysical Science, Graduate School of Science, Hiroshima University

[b]TOSHIBA Power System Company

[c]Hiroshima Synchrotron Radiation Center, Hiroshima University

The synchrotron radiation generated by a periodic linear undulator contains higher harmonics of integral multiple of fundamental harmonic in the spectrum. These higher harmonics are usually an obstacle to user's experiments. Therefore, to reduce higher harmonic contamination, such a user has to use many optical elements such as a monochromator, a band-pass filter, and a mirror to eliminate unwanted harmonics. However, such kind of beamline setup between an undulator and an end-station may cause a reduction of photon beam intensity. In order to ease such difficulties, quasi periodic undulator was developed in which higher harmonics appear at irrational positions instead of rational positions in the spectrum. A combination of a quasi-periodic undulator (QPU) and a single monochromator can provide purely monochromatic photon beam for end-users.

Until today, quasi periodic undulators used in all over the world are designed such that the peak magnetic field strength at certain positions representing the quasi-periodicity is reduced to introduce a smaller phase advance of photon wave at every QP position in an undulator. In this study, we design a new type quasi periodic undulator by increasing the magnetic field strength at every QP position to introduce a larger phase advance of photon wave. Fig.1 shows the magnetic structure of new QPU. The field variation of this undulator is presented in Fig.2. The spectral feature of this new QPU is shown in Fig.3. In the poster presentation, we introduce a new QPU model, and compare capabilities of new type QPU and conventional QPU by various conditions as shown in Fig.4 and Fig.5.

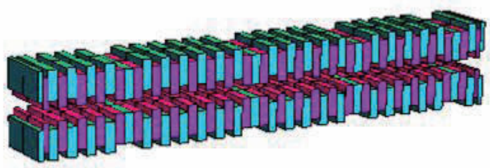

Fig.1. RADIA model of a new QPU

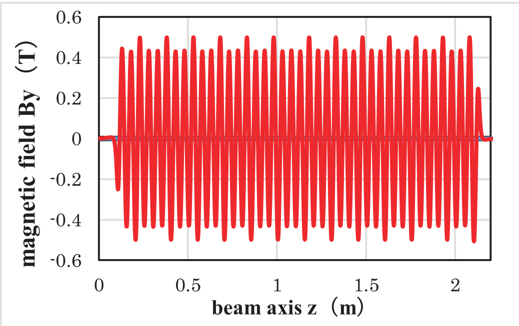

Fig.2. Magnetic field distribution of new QPU

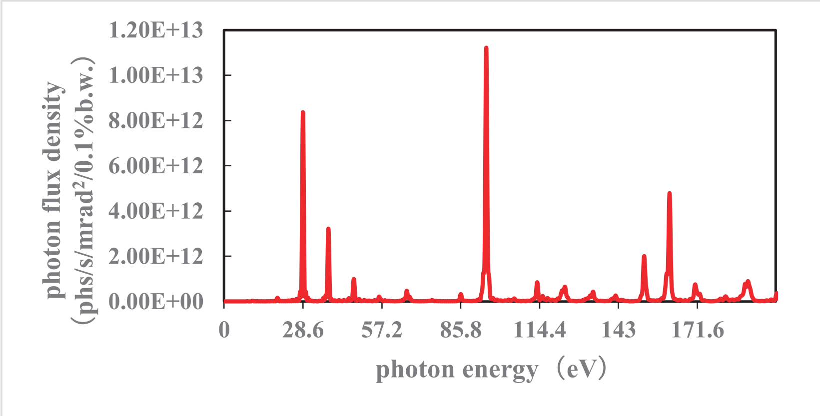

Fig.3. Radiation spectrum from new QPU calculated by the code SPECTRA

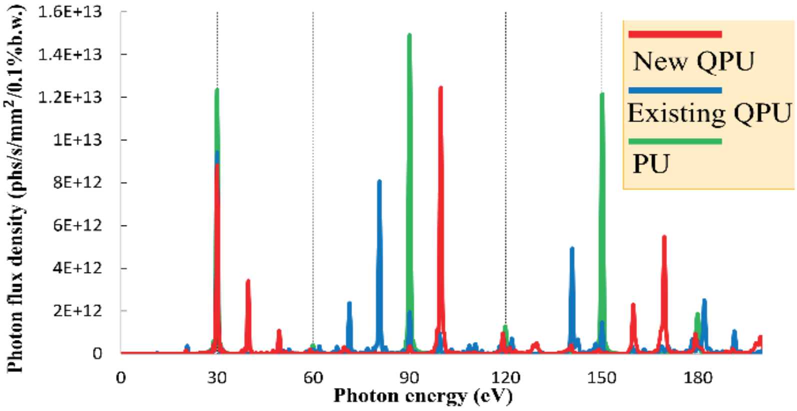

Fig.4: Comparison spectra of three different type of undulator ($E_{1st} = 30$ eV).

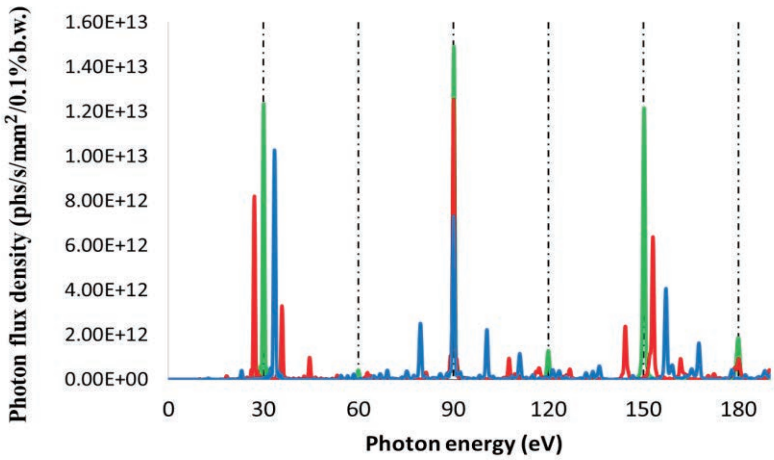

Fig.5: Comparison spectra of three different type of undulator ($E_{\sim 3rd} = 90$ eV).

REFERENCES

[1] S. Hashimoto and S. Sasaki, Nucl. Instr. Methods in Phys. Res. **A361**, 611, (1995).

[2] S. Sasaki, et.al, Proceedings of EPAC'98, p.2237, Stockholm, Sweden, 1998.

[3] S. Sasaki, Proceedings of IPAC'10. p.3141, Kyoto, Japan, 2010.

Research Activities

– Instrumental Developments –

Present status of VUV-laser based spin-ARPES system

Kazuki Sumida[a], Koji Miyamoto[b], Emilia Annese[b], Kazuaki Taguchi[a], Tomoki Yoshikawa[a], Yuki Okuda[b], Akio Kimura[a], Masaki Taniguchi[b], Hirofumi Namatame[b], and Taichi Okuda[b]

[a]*Graduate School of Science, Hiroshima University, 1-3-1 Kagamiyama, Higashi-Hiroshima 739-8526, Japan*
[b]*Hiroshima Synchrotron Radiation Center, Hiroshima University, 2-313 Kagamiyama, Higashi-Hiroshima 739-0046, Japan*

Keywords: Spin- and angle-resolved photoemission, VUV-Laser, VLEED

Spin- and angle-resolved photoemission spectroscopy (SARPES) is a very powerful tool to investigate the spin-dependent electronic structure in materials. Combination of the hemispherical electron analyzer with the state-of-the-art spin detector based on very low energy electron diffraction (VLEED) scheme utilizing the ferromagnetic target allows us to reveal the detailed spin texture of strong spin-orbit coupled materials such as Rashba systems, topological insulators and Weyl semimetals [1,2]. However, in the case of magnetic materials *e.g.* time-reversal symmetry breaking Weyl semimetals, it is difficult to get signals solely from a single magnetic domain, which is typically smaller than the light spot size. To overcome this problem a high spatial resolution is prerequisite. The use of the laser light source is one solution because it is easy to obtain the well-focused light with a small spot size. Furthermore, the highly efficient VLEED is advantageous to obtain the signal from the quite small spot with a diameter (< 10 μm). Therefore, in this apparatus, we combined VUV-laser light source with the VLEED spin detectors.

Figure 1 shows the schematic image of our VUV-laser based SARPES system. The system consists of hemispherical electron analyzer, double VLEED-type spin detector, motorized 5-axis goniometer (*i*-Gonio) with cryostat, the ultra-high vacuum chambers and VUV laser system. The hemispherical electron analyzer DA30-L has the horizontal and vertical electron deflectors (30 degrees full cone acceptance), which enables us to measure the spin integrated/resolved band dispersion and the constant energy contours without sample rotation by manipulator. This is a good advantage for the measurement of very small or the magnetic samples. Two VLEED spin detectors are attached orthogonally to the electron analyzer to make a vector analysis of spin polarization with three components in the Cartesian coordination system (P_x, P_y, and P_z) possible. This system equips two photon sources: (1) non-monochromatized He discharge lamp, and (2) photon energy tunable VUV laser (5.90 – 6.49 eV).

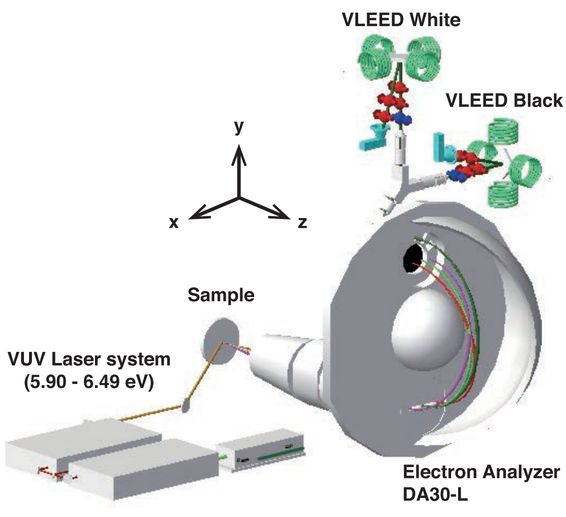

FIGURE 1. Schematic image of the VUV-laser based high efficiency SARPES system. The two VLEED detectors (VLEED White and VLEED Black) are orthogonally set each other.

In order to check the performance, we have performed ARPES and SARPES experiments for Bi(111) single crystal with He discharge lamp. Figs. 2(a) and 2(b) show the band dispersion of Bi(111) along $\overline{\Gamma K}$ and $\overline{\Gamma M}$ lines, respectively. Fig. 2(c) shows the constant energy contours acquired at several binding energies (E_B). The observed band dispersions and the hexagonal Fermi surface shape are consistent with the former results [3] though they are a little broadened due to an insufficient surface preparation. We have tried to measure spin polarizations in two ways. One is to acquire spin polarizations with deflector while the orientation of the sample surface fixed. The other is to measure spin polarizations by changing the surface orientation. Figures 2(d) and 2(e) show spin-resolved energy distribution curves (EDCs) obtained at ±7° from $\bar{\Gamma}$ point along $\overline{\Gamma K}$ and $\overline{\Gamma M}$ lines [white dashed lines in Figs. 2(a) and 2(b)]. The spin-up ($I_\uparrow$) and spin-down ($I_\downarrow$) intensities obtained from $I_\uparrow = (1 + P)I/2$ [$I_\downarrow = (1 - P)I/2$] with deflectors are denoted with open circles. The corresponding intensities denoted with filled circles are the results taken with sample rotation. Since these results are quite similar to each other, the results indicate that the data acquisition by deflectors works accurately as the conventional method with the sample rotation does. The effective Sherman function was also estimated to be ~0.25 by comparing to the previous study [1].

The installation of focusing lens and the modification of manipulator for high precision position control are now in progress for the measurement with higher spatial resolution.

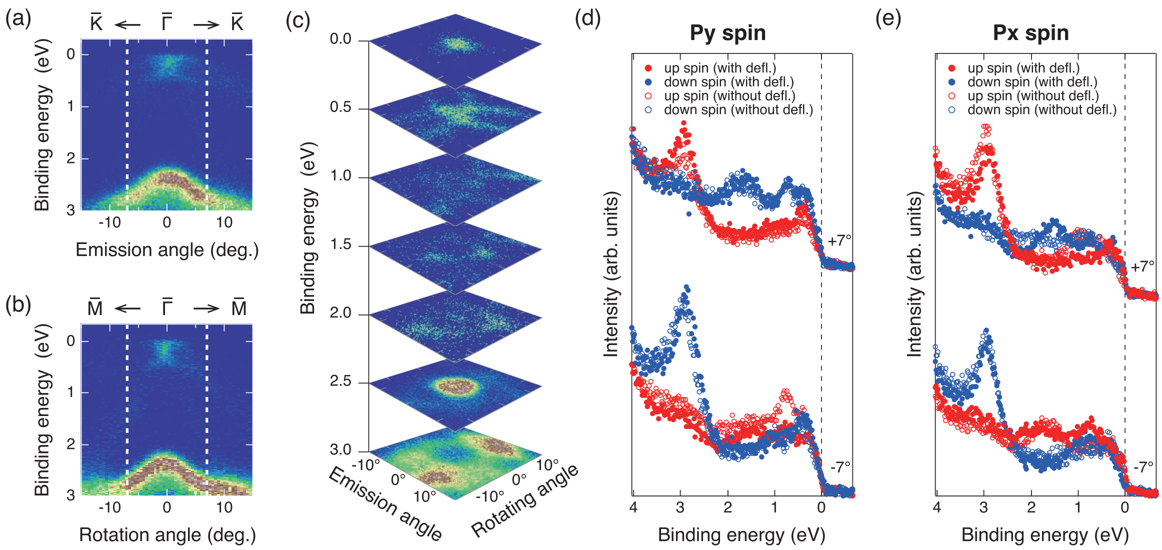

FIGURE 2. Band dispersions and spin-resolved intensities of bulk Bi(111) crystal with He discharge lamp. (a),(b) ARPES images along $\overline{\Gamma K}$ and $\overline{\Gamma M}$ lines, respectively. (c) Constant energy contours acquired at E_B = 0.0, 0.5, 1.0, 1.5, 2.0, 2.5 and 3.0 eV. (d),(e) Spin-resolved EDCs obtained with/without the deflector at ±7°from $\bar{\Gamma}$ point shown by dashed lines in (a) and (b).

REFERENCES

1. T. Okuda *et al.*, Rev. Sci. Instrum. **82**, 103302 (2011).
2. T. Okuda *et al.*, J. Electron Spectrosc. Relat. Phenom. **201**, 23 (2015).
3. C. R. Ast *et al.*, Phys. Rev. Lett. **87**, 177602 (2001).